IEEE Photonics Journal
An IEEE Photonics Society Publication

Open Access

Sparse Support Regression for Image Super-Resolution

Volume 7, Number 5, October 2015

Junjun Jiang
Xiang Ma
Zhihua Cai
Ruimin Hu

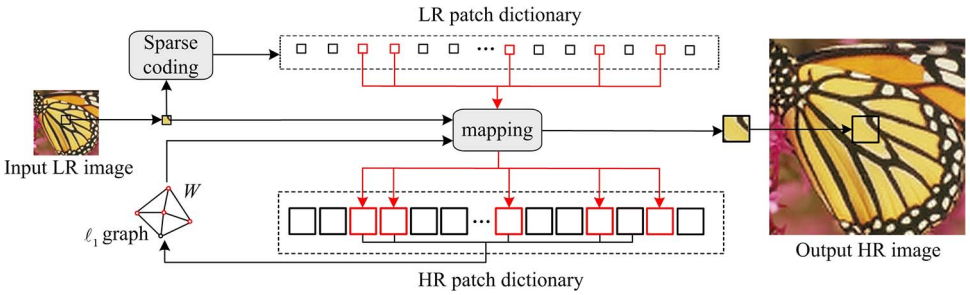

DOI: 10.1109/JPHOT.2015.2484287
1943-0655

IEEE photonics SOCIETY

IEEE

Sparse Support Regression for Image Super-Resolution

Junjun Jiang,[1,2] Xiang Ma,[3] Zhihua Cai,[1,2] and Ruimin Hu[4]

[1]School of Computer Science, China University of Geosciences, Wuhan 430074, China
[2]Hubei Key Laboratory of Intelligent Geo-Information Processing, China University of Geosciences, Wuhan 430074, China
[3]School of Information Engineering, Chang'an University, Xi'an 710064, China
[4]School of Computer, Wuhan University, Wuhan 430072, China

DOI: 10.1109/JPHOT.2015.2484287

Manuscript received July 23, 2015; revised September 25, 2015; accepted September 25, 2015. Date of publication September 29, 2015; date of current version October 12, 2015. This work was supported in part by the National Natural Science Foundation of China under Grant 61501413; by the China Fundamental Research Funds for the Central Universities under Grant 310824153508 (Chang'an University); by the Fundamental Research Funds for the Central Universities; by China University of Geosciences, Wuhan, China; and by the Open Foundation of Hubei Provincial Key Laboratory of Intelligent Robot under Grant HBIR201404. Corresponding author: X. Ma (e-mail: maxiang@chd.edu.cn).

Abstract: In most optical imaging systems and applications, images with high resolution (HR) are desired and often required. However, charged coupled device (CCD) and complementary metal-oxide semiconductor (CMOS) sensors may be not suitable for some imaging applications due to the current resolution level and consumer price. To transcend these limitations, in this paper, we present a novel single image super-resolution method. To simultaneously improve the resolution and perceptual image quality, we present a practical solution that combines manifold learning and sparse representation theory. The main contributions of this paper are twofold. First, a mapping function from low-resolution (LR) patches to HR patches will be learned by a local regression algorithm called sparse support regression, which can be constructed from the support bases of LR–HR dictionary. Second, we propose to preserve the geometrical structure of image patch dictionary, which is critical for reducing artifacts and obtaining better visual quality. Experimental results demonstrate that the proposed method produces high-quality results, both quantitatively and perceptually.

Index Terms: Optical imaging system, super-resolution, manifold learning, sparse representation.

1. Introduction

With the rapid progress in hand-held photographic mobile devices, images and videos are becoming increasingly more popular on the web, due to their rich content and easy perception. However, limited by optical imaging systems, most images exist as low-resolution (LR) versions degraded from the source. There is a huge need for improving the perceptual image quality, among which resolution enhancement technology is called super-resolution [1], [2]. Instead of imposing higher requirements on hardware devices and sensors, it can offer us high-resolution (HR) images in more detail economically. This paper focus on Single Image Super-Resolution (SISR) problem because of its potential effectiveness and flexibility for different applications [3]–[5].

1.1. Prior Work

Since SISR is inherently ill-posed as there are generally multiple HR images corresponding to the same LR image, accordingly, one has to rely on strong prior information, which is available either in the explicit form (e.g., Tikhonov regularization [6] and Total Variation regularization [7]) and/or in the implicit form [1], [8]. A few representative methods of such kind are summarized as follows.

Learning-based (or example-based) super-resolution has become a hot topic since it was first introduced by Freeman *et al.* in [1]. In this pioneering work, they model the relationship between LR and HR image patches by using Markov network. However, this approach is computationally intensive and sensitive to training examples. Another representative work for learning-based super-resolution was proposed by Chang *et al.* [9], which is based on Locally Linear Embedding (LLE) [10] manifold learning theory. It assumes that image patches in LR patch space and the corresponding HR one are located at two similar local geometries, and the HR patch could be generated as a linear combination of its K neighbor HR patches found in training database. In contrast to [1], Chang *et al.*'s method does not require a large number of samples and achieve good performance. Since then, there are a lot of different prior constraints have been introduced to regularize this ill-posed problem. Priors that are commonly exploited in SISR methods mainly include gradient profile prior [11], self-similarity prior [12], [13], coupled constraint [14]–[16], and locality regularization [17]–[19]

Recently, in [20] and [21], sparse coding is employed to perform for image super-resolution, which enforces corresponding LR and HR patches to share the same sparse representations. In their works, by enforcing sparsity regularization, LR patches are coded with respect to an over-complete LR dictionary, and the coefficients (i.e., the outcome of sparse coding process) are obtained to linearly combine corresponding HR counterparts to perform image super-resolution reconstruction. However, the constraint of *same sparse representation* in their approaches is too strong to achieve in practice [22].

1.2. Motivation and Contributions

In this paper, we present a manifold regularized regression framework for super-resolution. In the proposed framework, the regression relationship is learned from the LR–HR support spaces,[1] which are constructed based on sparse representation theory. Therefore, we call our proposed method Manifold regularized Sparse Support Regression, which is termed as MSSR for short. In MSSR, the *same sparse representation* assumption used in conventional sparse coding based methods is relaxed for LR–HR sparse support domain regression, which is flexible in using the information of local training samples [5], [25]. In addition, the proposed method simultaneously considers the manifold regularization, thus capturing the intrinsic geometrical structure of the dictionary. Part of our previous work has been published in [24]. Compared with previous image super-resolution approaches, our contributions can be summarized as follows:

- Compared with those sparse coding based methods [20], [21], which use the strong regularization of *same sparse representation* for learning, in this paper, the *same sparse representation* is relax for sparse support domain regression. Thus we can expect to give more flexibility to the learned mapping functions.
- Instead of learning a global mapping function from the entire training samples, we design to learn a data specific mapping function from its LR–HR sparse support domain, and thus the learned mapping function can be tuned towards specific input LR patch.
- Compared with those regression-based methods [17], [25], [26], which do not take the geometry of HR patch space into consideration, we explore the geometry of HR patch space and use the geometry to regularize the reconstructed HR patch space as well as the mapping function.

[1]Note that image patches have regular structures where accurate estimation of pixel values via regression is possible.

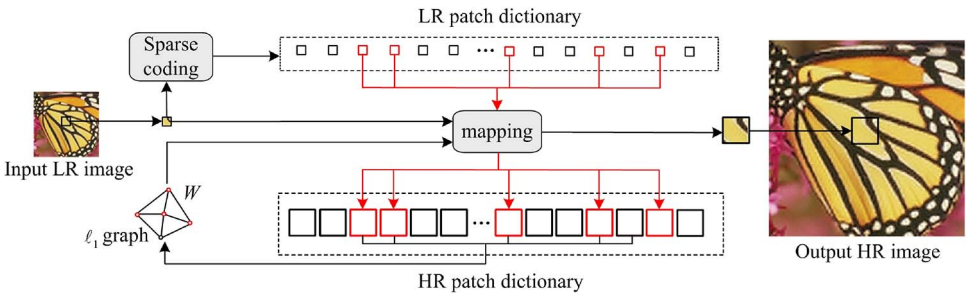

Fig. 1. Flowchart of the proposed method. Note that the red patches denote the sparse support domain of the input LR patch on dictionary, and we use the sparse graph of the HR sparse support domain to guide the construction of mapping function.

The remainder of this paper is organized as follows: In Section 2, we give the details of the proposed method. In Section 3, we give experiments and comparative results. We draw conclusions in Section 4.

2. Proposed Manifold Regularized Sparse Support Regression Method for Super-Resolution

2.1. Formulation and Overview of the Proposed Method

Given a set of LR and HR training image patch pairs, $\{(x_1, y_1), \ldots, (x_N, y_N)\} \subset R^d \times R^D$, d and D are dimensions of one LR patch and one HR patch, respectively. Define $X = [x_1, \ldots, x_N]$ and $Y = [y_1, \ldots, y_N]$, each column of which is a patch sample. Therefore, the matrixes X and Y can be viewed as the LR and HR patch dictionaries respectively. Considering that the manifold assumption (two manifolds spanned by the feature spaces of the LR and HR patches are locally similar) may not be tenable in practical [14], we learn a much more stable LR–HR mapping in the support domain for super-resolution, thereby, transforming super-resolution reconstruction to a regression problem. Our another important goal is to encode the geometry of HR patch manifold, which is much more credible and discriminated compared with that of the LR one [14], and preserve the geometry for the reconstructed HR patch space. This will ensure that the local geometric structure of the reconstructed HR patch manifold is consistent with that of the original HR one.

Based on the above discussions, our MSSR algorithm for image super-resolution should be equipped with two properties: i) The shared support of each LR patch and HR patch has an explicit regression relationship; ii) the local geometrical information on original HR patch dictionary is preserved.

Therefore, by integrating the data-fidelity term, the smooth term and the manifold regularized term, the objective function of MSSR method can be mathematically written as follows:

$$O_{\text{MSSR}} = \sum_i \varepsilon(P, x_i, y_i) + \alpha \|P\|_H^2 + \beta \|P\|_M^2 \tag{1}$$

where $\varepsilon(P, x_i, y_i)$ is a predefined loss function of support samples, $\|P\|_H^2$ is a regularization function measuring the smoothness of parameter P, and $\|P\|_M^2$ is an appropriate penalty term that should reflect the intrinsic structure of data. Here the regularization parameter α controls the complexity of function in ambient space while β controls the complexity of function along geodesics in intrinsic geometry of data space.

To provide an overview of MSSR method, we show the flowchart in Fig. 1. Given an input LR patch, we first obtain its LR–HR sparse support domains, and then use the graph structure of HR space to regularize the mapping function between LR and HR sparse support domains. Lastly, the output HR patch can be obtained by the learned mapping function. In the following,

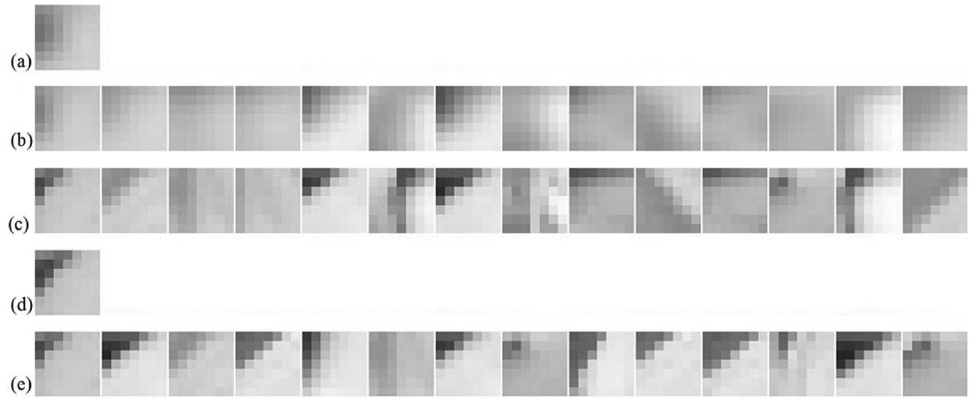

Fig. 2. Inconsistency between the LR and HR patch manifold spaces [26]. (a) Input LR image patch. (b) and (c) Fourteen closest LR patches and corresponding HR patches of (a). (d) Original HR patch of (a). (e) Fourteen closest HR patches of (d).

we will describe how we formulate MSSR with sparse support regression (see Section 2.2.) and manifold regularization (see Section 2.2.).

2.2. Sparse Support Regression

Instead of assuming that each pair of HR and LR patches has the *same sparse representation*, in our proposed MSSR method, this strong regularization of *same sparse representation* is relaxed for *sparse support regression*, in which the sparse coefficient vectors of one LR and HR patch pair share the *same support*, i.e., same indices of nonzero elements.

Given a set of LR and HR training patches (dictionary pairs), $\{(x_1, y_1), \ldots, (x_N, y_N)\}$, for an unseen LR patch x_t, we try to learn a mapping function $f(x, P) = Px$, from the LR patch to the corresponding HR one to minimize the following regularized cost function for the regression:

$$\varepsilon(P, x_i, y_i) = \sum_{i \in S} (Px_i - y_i)^2 \tag{2}$$

where S is the support of coding coefficients θ of unseen patch x_t on LR training patches X. The Compressive Sensing (CS) theory states that the observation signal can be reconstructed from a far fewer number of random measurements than the number of samples stipulated by Nyquist sampling theory. In recent years the sparsity-based regularization has led to promising results for various image restoration problems [20], [27]. In this paper, we introduce the spare constraint to coding coefficients θ

$$\hat{\theta} = \underset{\theta}{\operatorname{argmin}} \left\| x_t - X\theta \right\|_2 + \lambda_1 \|\theta\|_1 \tag{3}$$

where $\|\theta\|_1$ denotes ℓ_1 norm, and the regularization parameter λ_1 balances coding error of x_t and sparsity of θ. With an appropriate selection of the regularization parameter λ_1, we can get a good balance between the sparse approximation error of x_t and the sparsity of θ. The above λ_1 minimizing problem is well known as a basis pursuit problem. The solution of (3) can be achieved by convex optimization methods referring to [28].

The support of one vector is referring to the indices of nonzero elements in the vector. We denote the support of $\hat{\theta}$ as $S = \text{support}(\hat{\theta})$. Therefore, we can define the support sample sets as X_S and Y_S as $X_S = \{x_i | i \in S\}$ and $Y_S = \{y_i | i \in S\}$, respectively, we can rewrite (2) in the following matrix form:

$$\varepsilon(P, x_i, y_i) = \|PX_S - Y_S\|_F^2. \tag{4}$$

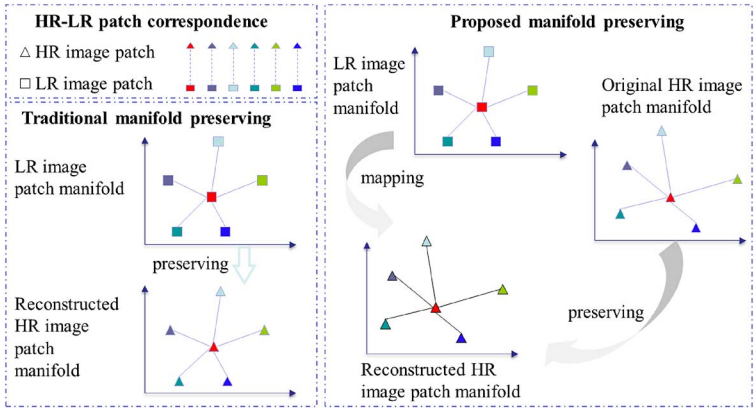

Fig. 3. Manifold preserving comparison between traditional method and our proposed method.

2.3. Manifold Regularization

This subsection targets on the second property, which is to preserve the local geometrical geometry of data. In previous manifold learning based super-resolution methods, such as neighbor embedding based super-resolution, they assume that the LR and HR manifold spaces share the similar local geometrical geometry. These algorithms all try to explore the neighborhood relationship of LR manifold space and preserve the learned neighborhood relationship for the target HR manifold space. However, since the image degeneration processing has information lost (i.e., the high-frequency details), the mapping between the LR image and the HR image is *one-to-many* in practical.

As illustrated in Fig. 2, for an input LR patch [see Fig. 2(a)], we searched a typical training database of approximately 100 000 patches to find the 14 closest LR patch samples in the LR patch space [see Fig. 2(b)]. Fig. 2(c) shows the HR patch samples corresponding to each of these LR patch samples; each of those looks fairly different from the other. We give the original HR patch in Fig. 2(d) and (e) is the 14 closest HR patch samples of Fig. 2(d), which can be seen as the true HR patches of the input LR input patch. This illustrates that i) inconsistency between the LR and HR patch manifold spaces and ii) that the local patch information of LR patch manifold alone is insufficient for super-resolution.

Therefore, in this paper, we try to preserve the intrinsic geometric structure of original HR patch manifold rather than LR patch manifold, which may be contaminated by image degeneration (e.g., blurring, down-sampling and noise), for the reconstructed HR patch manifold (as shown in the right part of Fig. 3). Compared with traditional manifold preserving methods (as shown in the left part of Fig. 3), which try to preserve the similar local geometric structure by imposing the local geometric of LR patch manifold on that of the reconstructed HR patch manifold, our motivation is to make the local geometric structure of reconstructed HR patch manifold and original HR patch manifold consistent.

Given a set of data points y_i, we can construct a nearest neighbor graph $G = (V, W)$, where each vertex represents a data point, $V = \{y_i\}$. A natural assumption here could be that if two points y_i and y_j are close in the intrinsic geometry of HR patch manifold space, their LR and HR versions x_i and x_j in the LR patch manifold space should be similar, i.e., should vary smoothly along the geodesics in the intrinsic geometry of original HR patch manifold. As described in (1), we use the $\|P\|_M^2$ to measure the smoothness of P along the geodesics in intrinsic geometry of data. When we consider the case that data is a compact sub-manifold, a natural choice for $\|P\|_M^2$ is

$$\|P\|_M^2 = \int_{y \in M} \|\nabla_M P\|^2 dy \tag{5}$$

where $\nabla_M P$ is the gradient of P along the manifold M. In reality, the data manifold M is unknown. Thus, $\|P\|_M^2$ in (5) cannot be computed. Recent studies on spectral graph theory [29] have demonstrated that $\|P\|_M^2$ can be discretely approximated through a nearest neighbor graph on a scatter of data points. How to define the edge weight matrix W is critical. Researchers have proposed various methods to measure the similarity between data points [30], [31], e.g., pair-wise distance based similarity and reconstruction coefficient based similarity. Since the former is suitable for discriminant analysis problems, such as recognition and clustering, it is mainly used for classification and recognition tasks. Alternatively, reconstruction coefficient based similarity is datum-adaptive and thus more suitable for image super-resolution. LLE [10] is one of the representative works for reconstruction coefficient similarity estimation.

Recently, some researchers have demonstrated that the sparse structure of one manifold can be explored by the ℓ_1 graph [31], resulting in many benefits for machine learning and image processing problems. Let y_i be the ith HR patch which is under consideration now. We want to identify its neighbors on the smooth manifold rather than the entire Euclidean space. On the smooth patch manifold space, the patch can be well sparsely approximated by a linear combination of a few nearby patches. Thus, it has a sparse representation over the support domain Y_S. For any HR patch y_i, it can be sparsely approximated by data matrix Y_S except y_i

$$\hat{W}_i = \underset{W_i}{\operatorname{argmin}} \|y_i - Y_S W_i\|_2 + \lambda_2 \|W_i\|_1, \qquad \text{s.t.} \quad W_{ii} = 0 \tag{6}$$

where W_i denotes the ith column of the edge weight matrix W whose diagonal elements are zeros, and λ_2 is the parameter balancing the coding error of y_i and the sparsity of W_i.

We preserve the geometry relation represented by W for the reconstructed HR patch manifold. When LR patch is transformed to the HR patch, we try to preserve geometry constraint from W for $PX_S W_i$. It can be gained by minimizing

$$\sum_{i \in S} \|Px_i - PX_S W_i\|_2^2 = \|PX_S - PX_S W\|_F^2 = \|PX_S(I - W)\|_F^2 \tag{7}$$

where I is an identity matrix.

2.4. MSSR Objective Function and Optimization

Considering above-mentioned two properties that we want to engage in, the objective function of our proposed MSSR is defined as

$$O_{\text{MSSR}} = \|PX_S - Y_S\|_F^2 + \alpha \|P\|_F^2 + \beta \|PX_S(I - W)\|_F^2. \tag{8}$$

Using matrix properties $\text{tr}(AB) = \text{tr}(BA)$, $\|A\|^2 = \text{tr}(AA^T)$, and $\text{tr}(A) = \text{tr}(A^T)$, we have

$$O_{\text{MSSR}} = \text{tr}\big(PX_S X_S^T P^T - PX_S Y_S^T - Y_S X_S^T P^T + Y_S Y_S^T\big) + \alpha \text{tr}(PP^T) + \beta \text{tr}\big(PX_S G X_S^T P^T\big) \tag{9}$$

where $G = (I - W)(I - W)^T$.

In order to minimize (9), we would like to take the derivative of O_{MSSR} with respect to P and set it to zero; thus

$$P\big(X_S X_S^T + \alpha I + \beta X_S G X_S^T\big) = Y_S X_S^T. \tag{10}$$

Then, we have

$$P = Y_S X_S^T \big(X_S X_S^T + \alpha I + \beta X_S G X_S^T\big)^{-1}. \tag{11}$$

Once a LR patch x_t comes, we can just project it onto P via

$$y_t = Px_t. \tag{12}$$

By integrating all the reconstructed HR patches according to the original position, the final HR image can be generated by averaging pixel values in the overlapping regions.

2.5. Iterative Back Projection

It is worth noting that the super-resolved HR image (denoted as Y_t^0) produced through a patch-wise strategy does not satisfy the reconstruction constraint exactly [20]. Accordingly, we try to take iterative back projection (IBP) as the post-processing to further enhance the quality of super-resolution results by above mentioned local patch based method. Given an observed LR image X_t, the global reconstruction constraint can be enforced to minimize the reconstruction error

$$E(Y_t, X_t) = \|X_t - DBY_t\|_2^2 \tag{13}$$

where D and B represent the down-sampling operator and blurring operator respectively. This global reconstruction constraint requires that the HR image should be as close as possible to the input LR image after smoothing and down-sampling. IBP can guide Y_t to be more consistent with the degradation model in (13), i.e.,

$$Y_t^* = \arg\min_{Y_t} \|X_t - DBY_t\|_2^2 + c\|Y_t - Y_t^0\|_2^2. \tag{14}$$

Here, the parameter c balances the prior and the back projection constraint. The solution to this optimization problem can be efficiently computed using gradient descent-based minimization

$$Y_t^{n+1} = Y_t^n + u\left[B^T D^T (X_t - DBY_t^n) + c(Y_t^n - Y_t^0)\right] \tag{15}$$

where Y_t^n is the estimation of HR image after the nth iteration, u is the step size of gradient descent, and the initial super-resolution result is Y_t^0. The entire procedure of MSSR is depicted in Algorithm 1.

Algorithm 1 Image Super-resolution via MSSR

1: **Input**: Training images and a LR test image X_t. The regularization parameters λ_1, λ_1, α and β
2: Training the LR and HR coupled dictionaries using the sparse coding method as in [20].
3: **for** each patch x_t of X_t **do**
4: Code x_t over X via ℓ_1 minimization to obtain the optimal coding coefficients $\hat{\theta}$ through Equation (3).
5: Obtain the sparse support, $S = \text{support}(\hat{\theta})$.
6: Obtain the support sample sets X_S and Y_S as $X_S = \{x_i | i \in S\}$ and $Y_S = \{y_i | i \in S\}$.
7: Construct the graph G on HR patch manifold and obtain the similarity matrix according to Equation (6).
8: Preserve the geometry W for the reconstructed HR patch manifold and obtain the mapping P according to Equation (11).
9: Compute the HR version of x_t via linear mapping according to Equation (15).
10: **end for**
11: Integrate all the reconstructed HR patches above and average pixel values in overlap regions to form the HR image Y_t^0.
12: Perform a back projection iteratively for Y_t according to Equation (12).
13: **Output:** HR target image Y_t.

3. Experimental Results

In this section, we verify the performance of MSSR method. We conduct experiments on five widely used test images as shown in Fig. 4, which are very representative for their contents are various, and they include the human, buildings, animals, grass, home, and so on.

Several state-of-the-art methods, such as Bicubic interpolation, Neighbor Embedding (NE) [9], Sparse Coding (SC) [20], and Local Learning based Regression (LLR) [17] are used as

Fig. 4. Gallery of test images used in our experiments. From left to right, they are named *barbara*, *foreman*, *house*,*lenna*, and *zebra* respectively.

TABLE 1

PSNR (dB), RMSE, and SSIM comparisons of different super-resolution methods

Images	**Bicubic**	**NE**	**SC**	**LLR**	**MSSR**
barbara	26.20 12.49 0.7543	26.49 12.08 0.7651	26.31 12.33 0.7689	26.51 12.05 0.7751	26.58 11.96 0.7810
foreman	29.64 8.41 0.9022	29.84 8.21 0.8874	30.59 7.54 0.9096	30.55 7.57 0.9083	31.00 7.19 0.9211
house	29.54 8.51 0.8564	29.70 8.35 0.8529	30.33 7.77 0.8586	30.25 7.83 0.8633	30.60 7.53 0.8756
lenna	31.73 6.61 0.8587	31.75 6.59 0.8555	32.85 5.81 0.8710	32.66 5.93 0.8710	33.07 5.66 0.8782
zebra	26.69 11.80 0.7946	27.31 10.99 0.8210	28.06 10.08 0.8250	28.08 10.05 0.8318	28.49 9.60 0.8417
Average	28.76 9.56 0.8332	29.02 9.24 0.8364	29.63 8.70 0.8466	29.61 8.69 0.8499	29.95 8.39 0.8595
Improvement	**1.19** **1.17** **0.0263**	**0.93** **0.85** **0.0231**	**0.32** **0.31** **0.0129**	**0.34** **0.30** **0.0096**	— — —

comparison baselines. Peak Signal to Noise Ratio (PSNR), Root Mean Square Error (RMSE), and Structural Similarity (SSIM) [32] indices are adopted to evaluate the objective quality of super-resolution results. Since human eyes are more sensible to the change of luminance, hence, super-resolution reconstruction is only performed on the luminance component, and the simple Bicubic interpolator is used for chromatic components.

To extract the high-frequency information of LR images, four directions of gradients (two horizontal directions and two vertical directions) are used as input features. The magnification factor is 3, the size of LR patches is set to 3 $\times$ 3, and the size of HR patches is set to 9 $\times$ 9.50 000 LR and HR training patch pairs are randomly chosen from training images used in [20], which has no relation with the test images used in our experiments, for NE [9] and LLT [17] and the coupled dictionaries with 1024 elements [20] respectively. The neighborhood number of NE [9] is set to 10 and the sparsity parameter of SC is set to 0.1. For the sake of fairness, we use the same trained dictionary for SC [20] and MSSR. For MSSR, the regularization parameters λ_1, λ_2, α, and β are empirically set to 0.1 , 0.15, 0.3, and 10, respectively.

PSNR (dB), RMS,E and SSIM of all five different test images are reported in Table 1. It can be seen from this table that MSSR method achieves the best in terms of PSNR, RMSE and SSIM. MSSR outperforms Bicubic interpolation, NE [9], SC [20], and LLR [17] in all cases, which validates the necessity and effectivity of sparse support regression and manifold geometric preservation.

Fig. 5 shows the visual results of different super-resolution algorithms. All of the learning-based super-resolution methods outperform Bicubic interpolation in terms of visual plausibility. Note that the proposed algorithm performs visually much better than Bicubic interpolation, having less visual artifacts and producing sharper results. Compared with other learning-based

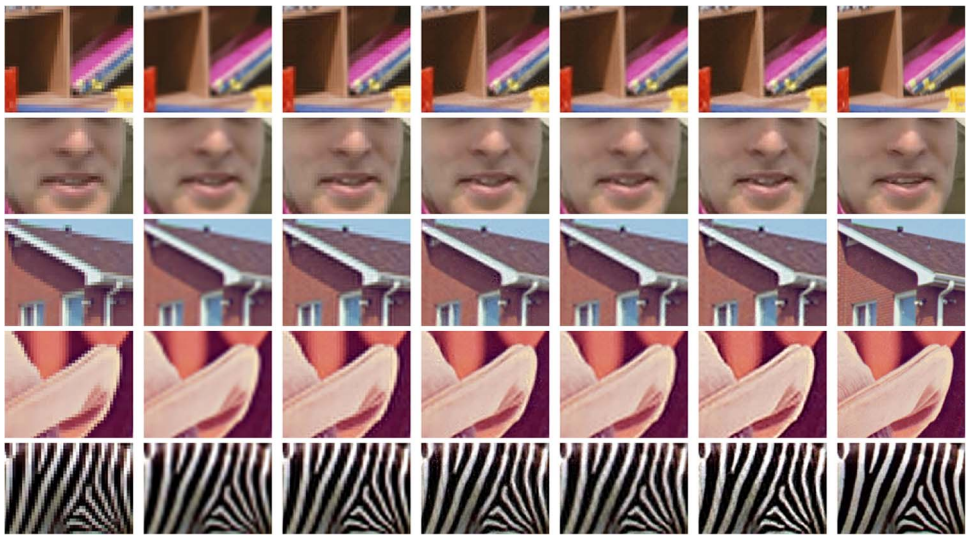

Fig. 5. Super-resolution results of different methods. The top row to the bottom row are the local magnification of *barbara*, *foreman*, *house*, *lenna*, and *zebra*, respectively.

super-resolution methods, the proposed algorithm provides more image details with improved objective values. The results of NE [9] method are sharp in textures. However, unpleasant artifacts and tiny block effects are also introduced as shown in *foreman* and *lenna*. SC [20] method uses the sparseness prior to regularize the HR image, which suppresses the high frequency details in the texture region but introduces some noise as shown in *barbara*, *house*, and *zebra* images. This is mainly due to the difficulty to learn a universal coupled LR and HR dictionary that can represent various LR and HR structure pairs. The result of locality prior method (LLR [17]) shown in the fifth column is sharp along salient edges. However, the texture detail is blurry and there are some jaggy artifacts and ringing artifacts. Our result in the sixth column is sharp both along edges and in textural regions. We owe the superiority of the proposed method to manifold constrained local sparse regression, which is more powerful and flexible to describe different image patterns.

We further compare the proposed method with comparison methods in term of CPU time. Fig. 6 shows the CPU time spent on each test image performed using Matlab 7.14 (R2012a) on an Inter(R) core(TM)i3 CPU with 3.20 GHz and 4G memory PC at Windows platform. Bicubic interpolation is the fastest and need only around 10^{-2} seconds for each image. NE [9] and LLT [17] learn the LR–HR relationship based on raw training samples with large size (50,000 LR and HR patch pairs), and the time spent on each test image is around 10^3 seconds due to k-NN search in large-scale dataset. By learning a compact dictionary (1024 elements), SC [20] and MSSR require much less time in comparing with NE [9] and LLT [17]. However, these approaches are difficult for practical applications where real-time or near real-time performance must guarantee. Despite this, thanks to the independence of reconstruction of each target HR patch, we could still make use of the parallel computation technology to accelerate the super-resolution algorithms.

4. Main Findings and Future Directions

In order to overcome the hardware limitations of optical system, in this paper we develop a novel single image super-resolution method, namely Manifold regularized Sparse Support Regression (MSSR), which simultaneously considers the manifold geometrical structure of patch manifold space and the support of the corresponding sparse coefficients. The support information as well as the geometrical structure information of data manifold is incorporated into MSSR

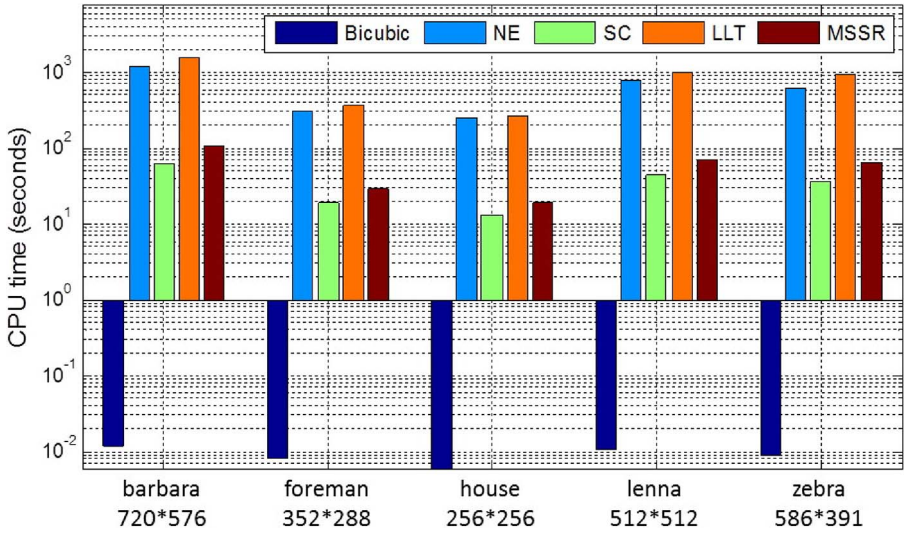

Fig. 6. Comparisons of CPU time between the proposed method and the comparison method.

model. We design a novel sparse regression algorithm having both reconstruction and generalization properties, which can enhance the learning performance. It is experimentally shown that MSSR method can produce more faithful details and higher objective quality in comparison to the other state-of-the-art super-resolution approaches. Extending the current linear model to the non-linear case will be our further work. In addition, we may introduce some reasonable priors [27], [33] to suppress artifact of super-resolved image.

Acknowledgment

The authors would like to thank the anonymous reviewers for their valuable suggestions.

References

[1] W. Freeman, E. Pasztor, and O. Carmichael, "Learning low-level vision," *Int. J. Comput. Vis.*, vol. 40, no. 1, pp. 25–47, Oct. 2000.
[2] S. C. Park, M. K. Park, and M. G. Kang, "Super-resolution image reconstruction: A technical overview," *IEEE Signal Process. Mag.*, vol. 20, no. 3, pp. 21–36, May 2003.
[3] X. Ma, J. Zhang, and C. Qi, "Hallucinating face by position-patch," *Pattern Recognit.*, vol. 43, no. 6, pp. 2224–2236, Jun. 2010.
[4] J. Jiang, R. Hu, Z. Wang, and Z. Han, "Face super-resolution via multilayer locality-constrained iterative neighbor embedding and intermediate dictionary learning," *IEEE Trans. Image Process.*, vol. 23, no. 10, pp. 4220–4231, Oct. 2014.
[5] T. Peleg and M. Elad, "A statistical prediction model based on sparse representations for single image super-resolution," *IEEE Trans. Image Process.*, vol. 23, no. 6, pp. 2569–2582, Jun. 2014.
[6] A. N. Tikhonov and V. Y. Arsenin, "Solutions of ill-posed problems," *Math. Comput.*, vol. 32, no. 5, pp. 491–491, Oct. 1978.
[7] L. I. Rudin, S. Osher, and E. Fatemi, "Nonlinear total variation based noise removal algorithms," *Phys. D, Nonlinear Phenom.*, vol. 60, no. 1–4, pp. 259–268, Nov. 1992.
[8] Z. Lin and H.-Y. Shum, "Fundamental limits of reconstruction-based superresolution algorithms under local translation," *IEEE Trans. Pattern Anal. Mach. Intell.*, vol. 26, no. 1, pp. 83–97, Jan. 2004.
[9] H. Chang, D. Yeung, and Y. Xiong, "Super-resolution through neighbor embedding," in *Proc. IEEE Conf. Comput. Vis. Pattern Recog.*, 2004, vol. 1, pp. 275–282.
[10] S. T. Roweis and L. K. Saul, "Nonlinear dimensionality reduction by locally linear embedding," *Science*, vol. 290, no. 5500, pp. 2323–2326, Dec. 2000.
[11] J. Sun, J. Sun, Z. Xu, and H.-Y. Shum, "Image super-resolution using gradient profile prior," in *Proc. IEEE CVPR*, 2008, pp. 1–8.
[12] Z. Zhu, F. Guo, H. Yu, and C. Chen, "Fast single image super-resolution via self-example learning and sparse representation," *IEEE Trans. Multimedia*, vol. 16, no. 8, pp. 2178–2190, Dec. 2014.
[13] K. Zhang, X. Gao, D. Tao, and X. Li, "Single image super-resolution with multiscale similarity learning," *IEEE Trans. Neural Netw. Learn. Syst.*, vol. 24, no. 10, pp. 1648–1659, Oct. 2013.
[14] X. Gao, K. Zhang, D. Tao, and X. Li, "Joint learning for single image super-resolution via coupled constraint," *IEEE Trans. Image Process.*, vol. 21, no. 2, pp. 469–480, Feb. 2012.

[15] C. Chen and J. E. Fowler, "Single-image super-resolution using multihypothesis prediction," in *Conf. Rec. 46th ASILOMAR Conf. Signals, Syst. Comput.*, 2012, pp. 608–612.
[16] J. Jiang, R. Hu, Z. Wang, Z. Han, and J. Ma, "Facial image hallucination through coupled-layer neighbor embedding," *IEEE Trans. Circuits Syst. Video Technol.*, DOI:10.1109/TCSVT.2015.2433538, 2015.
[17] Y. Tang, P. Yan, Y. Yuan, and X. Li, "Single-image super-resolution via local learning," *Int. J. Mach. Learn. Cybern.*, vol. 2, no. 1, pp. 15–23, Mar. 2011.
[18] J. Jiang, R. Hu, Z. Wang, and Z. Han, "Noise robust face hallucination via locality-constrained representation," *IEEE Trans. Multimedia*, vol. 16, no. 5, pp. 1268–1281, Aug. 2014.
[19] J. Jiang, R. Hu, C. Liang, Z. Han, and C. Zhang, "Face image super-resolution through locality-induced support regression," *Signal Process.*, vol. 103, pp. 168–183, Oct. 2014.
[20] J. Yang, J. Wright, T. Huang, and Y. Ma, "Image super-resolution via sparse representation," *IEEE Trans. Image Process.*, vol. 19, no. 11, pp. 2861–2873, Nov. 2010.
[21] Y. Sun, G. Gu, X. Sui, Y. Liu, and C. Yang, "Single image super-resolution using compressive sensing with a redundant dictionary," *IEEE Photon. J.*, vol. 7, no. 2, pp. 1–11, Apr. 2015, Art. ID. 6900411.
[22] Y. Liang, "Semi-coupled dictionary learning with applications to image super-resolution and photo-sketch synthesis," in *Proc. IEEE Conf. Comput. Vis. Pattern Recog.*, 2012, pp. 2216–2223.
[23] K. Jia, X. Wang, and X. Tang, "Image transformation based on learning dictionaries across image spaces," *IEEE Trans. Pattern Anal. Mach. Intell.*, vol. 35, no. 2, pp. 367–380, Feb. 2013.
[24] J. Jiang, R. Hu, Z. Wang, Z. Han, and S. Dong, "Manifold regularized sparse support regression for single image super-resolution," in *Proc. IEEE Int. Conf. Acoust., Speech, Signal Process.*, May 2013, pp. 1429–1433.
[25] K. I. Kim and Y. Kwon, "Single-image super-resolution using sparse regression and natural image prior," *IEEE Trans. Pattern Anal. Mach. Intell.*, vol. 32, no. 6, pp. 1127–1133, Jun. 2010.
[26] J. Jiang, R. Hu, Z. Han, and T. Lu, "Efficient single image super-resolution via graph-constrained least squares regression," *Multimedia Tools Appl.*, vol. 72, no. 3, pp. 2573–2596, Oct. 2014.
[27] M. F. Tappen, B. C. Russell, and W. T. Freeman, "Exploiting the sparse derivative prior for super-resolution and image demosaicing," in *Proc. IEEE Workshop Stat. Comput. Theories Vis.*, 2003, pp. 1–24.
[28] H. Lee, A. Battle, R. Raina, and A. Y. Ng, "Efficient sparse coding algorithms," in *Proc. NIPS*, 2007, pp. 801–808.
[29] S. Yan, D. Xu, B. Zhang, and H. J. Zhang, "Graph embedding: A general framework for dimensionality reduction," in *Proc. IEEE Conf. Comput. Vis. Pattern Recog.*, 2005, pp. 830–837.
[30] B. Cheng, J. Yang, S. Yan, Y. Fu, and T. S. Huang, "Learning with l1-graph for image analysis," *IEEE Trans. Image Process.*, vol. 19, no. 4, pp. 858–866, Apr. 2010.
[31] C. Ding, X. He, and H. D. Simon, "On the equivalence of nonnegative matrix factorization and spectral clustering," in *Proc. SIAM Int. Conf. Data Mining*, 2005, pp. 606–610.
[32] Z. Wang, A. Bovik, H. Sheikh, and E. Simoncelli, "Image quality assessment: From error visibility to structural similarity," *IEEE Trans. Image Process.*, vol. 13, no. 4, pp. 600–612, Apr. 2004.
[33] Y. W. Tai, S. Liu, M. S. Brown, and S. Lin, "Super resolution using edge prior and single image detail synthesis," in *Proc. IEEE Conf. Comput. Vis. Pattern Recog.*, 2010, pp. 2400–2407.